Improved Ronchi test with extended source

Joseph Braat and Augustus J. E. M. Janssen

Philips Research Laboratories, Professor Holstlaan 4, 5656 AA Eindhoven, The Netherlands

Received April 27, 1998; revised manuscript received August 17, 1998; accepted September 3, 1998

A modified Ronchi test with an extended source is presented. By the use of a matched pair of source grating and Ronchi grating, a pure shearogram between two shifted wave fronts is obtained, and the extra interference with other disturbing grating orders is largely suppressed by the use of a specific grating layout. © 1999 Optical Society of America [S0740-3232(99)00501-3]

OCIS codes: 050.1950, 220.4810, 030.1640, 050.1380, 100.2960, 120.3180, 070.2580.

1. INTRODUCTION

The Ronchi test has been the subject of numerous publications; both the original ray optics approach and the more complicated physical optics explanation have been described. An interesting paper has been written by the inventor himself,[1] and extensive reviews are found in Refs. 2–5.

In Fig. 1 the elementary Ronchi setup is shown. To increase the optical throughput in the case of an incoherent source, the source point is replaced by an extended source that is covered by a source grating conjugate in position and magnification with the Ronchi grating. The ray optics approximation is valid when coarse gratings are used. The maxima of the projected Ronchi pattern are given by the conditions

$$\Delta x_t'(X, Y) = m_x p_x', \qquad \Delta y_t'(X, Y) = m_y p_y', \qquad (1)$$

where (X, Y) are the coordinates on the wave front and (x', y') are the coordinates in the plane of the Ronchi grating. $p_{x'}'$ and $p_{y'}'$ are the periods associated with the Ronchi gratings for analysis in the x' and y' directions. $\Delta x_t'$ and $\Delta y_t'$ are the lateral aberration components of a ray on the wave front at the coordinates (X, Y); m_x and m_y are integers.

As such, the method is not adapted to the measurement of the small residual aberrations of a system close to the diffraction limit. To increase the sensitivity of the method, the pitch of the gratings has to be reduced; however, the diffraction effects are not negligible in this case, and they require the more complete physical optics analysis. The pattern on the screen D in the case of a higher-frequency grating has been depicted in Fig. 2; diffracted beams up to second order are shown, each shifted over a $\Delta X_m'$ equal to $m\lambda R'/p'$ (m is the order number, and R' is the distance from the Ronchi grating G_R to the screen D). The Ronchi grating interferometer with the use of a point source shows an interference pattern in each overlapping region of two orders. In the case of a Ronchi test with an extended grating source, the interference phenomenon is more intricate; one generally refers to the Zernike–van Cittert theorem,[6] which states that the coherence function over the entrance pupil of the optics under test is given by the Fourier transform of the intensity distribution function of the extended source. In the case of a source grating, periodic coherence peaks are present in the entrance pupil, corresponding to the far-field diffraction orders of the source grating. Applied to the Ronchi grating interferometer, the mutual interferences caused by the Ronchi grating are now limited to orders that have a shift proportional to the separation of the spatially periodic coherence peaks in the illuminated entrance pupil.[5] One of the consequences is that the orders $+1$ and -1 do not interfere if the illumination is done with a 50% duty-cycle source grating, because the second-order coherence peaks then have disappeared. In Section 2 we will analyze in more detail the Ronchi interferogram on the detection screen D in the presence of an arbitrary source intensity function.

The main problem in evaluating a Ronchigram is that several interference patterns overlap and the interpretation of the composite pattern is difficult (see Fig. 2). In Ref. 7 spatial filtering in a defocused plane is used to select only two orders. This method requires high-frequency gratings, and the spatial filtering is cumbersome in a Ronchi test with an extended source. The multiple-interference problem can also be tackled by attributing a value $\leqslant\lambda/\mathrm{NA}$ to the period p' so that only the zero and first orders overlap in well-separated regions (NA is the numerical aperture of the beam leaving the exit pupil). The disadvantage of this solution is that p' tends to very small values if a high-aperture optical system needs to be tested. Another disadvantage is that the reconstruction of a wave-front aberration is optimum if the shear ratio, defined as $s = \Delta X_1'/(2\rho')$, is definitely less than 0.50 (Ref. 8) ($2\rho'$ is the diameter of a diffraction order). For these reasons we need to devise a Ronchi configuration with a low shear ratio that is capable of yielding unambiguously reconstructed wave fronts.

In the remainder of this paper, we show how the Ronchi test can be adapted to a shear ratio below 50% without stumbling into the multiple-interference problem sketched above. In Section 2, after a theoretical introduction, we describe the principle of the improved Ronchi test. In Section 3 we show how the choice of a specific grating profile can lead to a drastic reduction of the unwanted interferences at low shear ratios.

0740-3232/99/010131-10$15.00

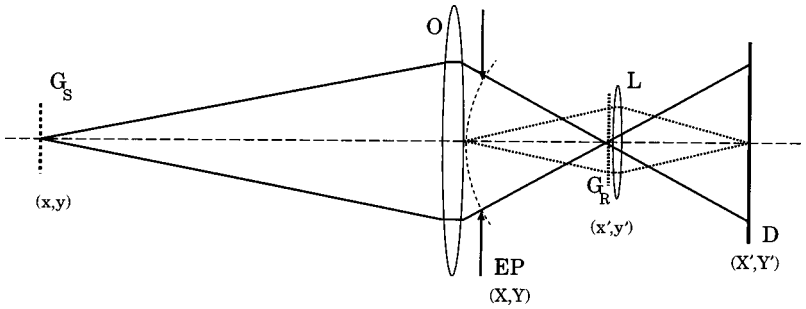

Fig. 1. Ronchi test. An extended source covered by a grating structure G_S is focused by the optics O to be measured onto the corresponding Ronchi grating G_R. An auxiliary lens L is inserted to image the exit pupil EP of the optics onto the detection screen D. In the ray optics approximation, the local fringe deformation is given by the transverse aberration on G_R of a ray originating from the corresponding point in EP.

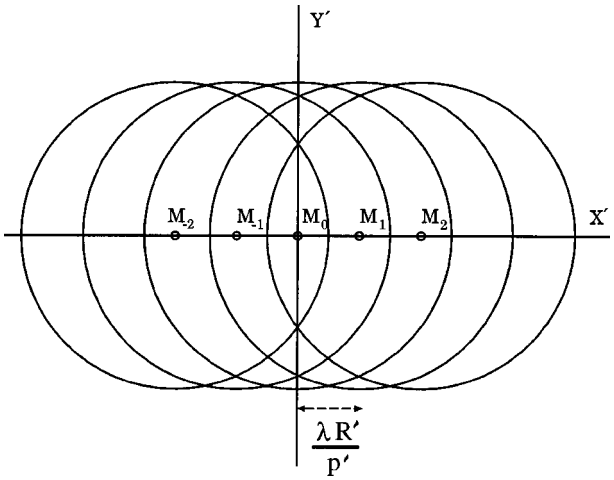

Fig. 2. Far-field pattern projected onto the detection screen D [coordinates (X', Y') in the case of a point source]. The pattern is the superposition of the diffraction orders generated by the Ronchi grating G_R. The spacing between the centers of the diffraction orders is determined by the wavelength λ of the light, the grating period p', and the distance R' between the grating plane and D.

2. PRINCIPLE OF THE IMPROVED RONCHI TEST

In this section we first give a more detailed analysis of the Ronchi test when one is using an extended source. In the second part of this section, we discuss the necessary modifications that lead to the improved version of the Ronchi test.

In Fig. 3 a source point Q belonging to an extended source emits a spherical wave toward the optics under test, O, here represented by a simple lens. The (aberrated) image point is located at Q′ in the plane where the Ronchi grating is located. The focused wave is split by the grating into a number of diffraction orders, which partly overlap. In Fig. 3 the zero order (solid circle) and, e.g., a first order (dotted–dashed circle) are present on the screen D. The state of interference in the overlap region of both circles depends on two factors. First, the aberration of the focused wave determines the phase in each point of the overlap region, depending on the lateral shear induced by the Ronchi grating. Second, the position x' of the imaged point Q′ with respect to the lines of the Ronchi grating determines an extra overall phase shift $\phi_m = 2\pi m x'/p'$ between the zero order and a diffracted order with order number m. This overall phase shift ϕ_m limits the possible extent in the x direction of an extended incoherent source that contributes a large number of individual interference patterns, all with varying values of ϕ_m. As a rule of thumb, we require that the value of $|\phi_m|$ not exceed $\pi/2$ to avoid a smear-out of the composite interference pattern, and this limits the incoherent source size to $p'/(2\beta')$, taking into account the magnification β' of the optics. The source size can be extended by blocking the source sections that give rise to destructive interference patterns, and this leads to the introduction of a source grating that is conjugate in period with the analyzing Ronchi grating. The final tolerable extent of the source is then limited by the isoplanatic region of the optics under test, over which the aberrational change of the imaging pencils is less than, e.g., $\lambda/100$.

A. Image Formation of a Ronchigram

To calculate the intensity pattern on the detection screen D, we start with a single source point in the source plane S (see Fig. 4); the coordinates of the particular source point are (x_0, y_0), and the complex amplitude of the wave on the exit pupil sphere EP of the optical system is given by

$$A(X, Y; x_0, y_0) = [I(x_0, y_0)]^{1/2}\exp\left[\frac{2\pi i}{\lambda R_0}(x_0X + y_0Y)\right] \times f(X, Y; x_0, y_0), \quad (2)$$

where $I(x_0, y_0)$ is the intensity distribution in the source plane.

The function $f(X, Y; x_0, y_0)$ is the pupil function of the optical system to be tested; formally, it also depends on the position (x_0, y_0) of the source point. The linear exponential factor is required because, in general, the spherical wave is obliquely incident on the entrance pupil of the optical system O.

The complex amplitude in the plane of the Ronchi grating is obtained by Fourier-transforming the expression for $A(X, Y)$:

$$B(x', y'; x_0, y_0) = [I(x_0, y_0)]^{1/2}\int\int \exp\left\{\frac{2\pi i}{\lambda}\left[X\left(\frac{x_0}{R_0} - \frac{x'}{R}\right) + Y\left(\frac{y_0}{R_0} - \frac{y'}{R}\right)\right]\right\} f(X, Y)\mathrm{d}X\mathrm{d}Y, \quad (3)$$

where we have dropped the dependency of the pupil function f on the source coordinates. This implies that the source extent should be limited to the isoplanatic region of the optical system O.

The amplitude distribution $B(x', y')$ after the Ronchi grating is obtained by multiplying this function by the amplitude transmission function $t(x'-\Delta x', y')$ of the grating. The shift $\Delta x'$ in the position of the grating makes it possible to influence the phase of a diffraction order of the grating.

The propagation of the light through the lens L toward the detection screen D is accounted for by a second Fourier transform:

$$A'(X', Y'; x_0, y_0) = \iint t(x' - \Delta x', y')B(x', y') \times \exp\left[\frac{-2\pi i}{\lambda R'}(x'X' + y'Y')\right]dx'dy'. \quad (4)$$

Inserting the expression for $B(x', y')$ from Eq. (3), we obtain

$$A'(X', Y'; x_0, y_0) = \iiiint [I(x_0, y_0)]^{1/2} \times f(X, Y)\exp\left[\frac{2\pi i}{\lambda R_0}(Xx_0 + Yy_0)\right]t(x' - \Delta x', y') \times \exp\left\{\frac{-2\pi i}{\lambda}\left[x'\left(\frac{X'}{R'} + \frac{X}{R}\right) + y'\left(\frac{Y'}{R'} + \frac{Y}{R}\right)\right]\right\}dx'dy'dXdY. \quad (5)$$

The function $t(x', y')$ is associated with the Ronchi grating G_R (see Fig. 4); we suppose that this function is periodic in x' with period p' and that it has an infinite extent. Its Fourier transform with respect to the x' coordinate then yields a series of δ functions. In the y' direction, we permit a geometry that is more general than that of a standard rectilinear grating: the grating cross section may depend on the vertical coordinate y'. In this case the Fourier transform of $t(x', y')$ can be written as a series of products of equidistant δ functions along the X' axis and Y'-dependent functions whose shape depends on the order number m of a particular δ function:

$$\mathrm{FT}\{t(x' - \Delta x', y')\} = \sum_m \exp\left(2\pi i m \frac{\Delta x'}{p'}\right) \times \delta\left(X' - \frac{m\lambda R'}{p'}\right)\tau_m\left(\frac{Y'}{R'}\right), \quad (6)$$

where the functions $\tau_m(Y')$ take into account the specific profile of an mth diffraction order in the Y' direction.

Using Eq. (6) in the expression for $A'(X', Y'; x_0, y_0)$ and performing the integration over the δ functions, we obtain, apart from a constant factor, the following:

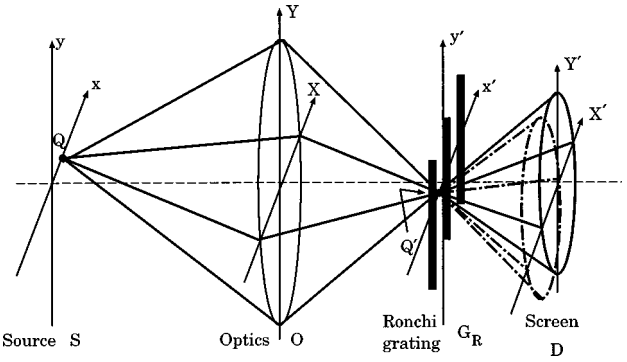

Fig. 3. Impression of the interference pattern produced by a single coherent source point Q on the detection screen D. In the plane of the Ronchi grating, a lens (not shown) takes care of the imaging of the exit pupil of the optics under test onto D.

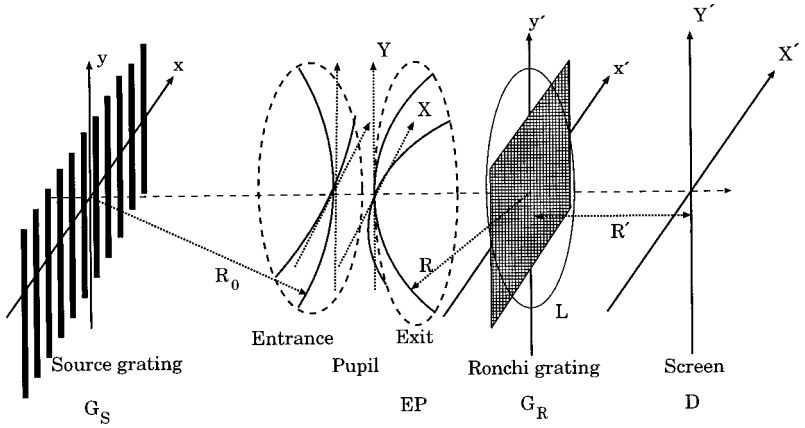

Fig. 4. Schematic layout of the Ronchi test showing the definition of the coordinates used in the analysis. The Ronchi grating is followed by a lens L that images the exit pupil of the optical system onto the detection screen D. The axial distances from the source to the entrance pupil, from the exit pupil to the Ronchi grating, and from the Ronchi grating to the detection screen are R_0, R, and R', respectively. To simplify the analysis, we fix the pupil magnification of the optical system to +1.

$$
\begin{aligned}
&A'(X', Y'; x_0, y_0) \\
&\quad = \sum_m [I(x_0, y_0)]^{1/2} \iint f(X, Y) \\
&\qquad \times \exp\left[\frac{2\pi i}{\lambda R_0}(Xx_0 + Yy_0)\right] \delta\left(\frac{X'}{R'} + \frac{X}{R} - \frac{m\lambda}{p'}\right) \\
&\qquad \times \tau_m\left(\frac{Y'}{R'} + \frac{Y}{R}\right) \exp\left(2\pi i m \frac{\Delta x'}{p'}\right) \mathrm{d}X\mathrm{d}Y \\
&\quad = \sum_m [I(x_0, y_0)]^{1/2} \exp\left\{\frac{2\pi i m}{p'}\left[\Delta x' - \left(\frac{R}{R_0}\right)x_0\right]\right\} \\
&\qquad \times \int f\left(-\frac{R}{R'}X' - \frac{m\lambda R}{p'}, Y\right) \tau_m\left(-\frac{Y'}{R'} - \frac{Y}{R}\right) \\
&\qquad \times \exp\left[-\frac{2\pi i}{\lambda R_0}\left(\frac{R}{R'}x_0X' - Yy_0\right)\right] \mathrm{d}Y. \qquad (7)
\end{aligned}
$$

The intensity distribution on the detection screen that is due to a source point at (x_0, y_0) is given by the squared modulus of $A'(X', Y'; x_0, y_0)$. The total intensity that is due to the extended source is obtained by integrating over the source intensity while taking into account the presence of the source grating with intensity transmittance function $T(x_0, y_0)$. These operations yield our final expression:

$$
\begin{aligned}
I_{\mathrm{tot}}(X', Y') = \sum_m \sum_{m'} &\iint I(x_0, y_0) T(x_0, y_0) \\
&\times \exp\left\{2\pi i\left(\frac{m - m'}{p'}\right)\left[\Delta x' - \left(\frac{R}{R_0}\right)x_0\right]\right\} \\
&\times \iint \mathrm{d}Y_1 \mathrm{d}Y_2 \, f\left(-\frac{R}{R'}X' - \frac{m\lambda R}{p'}, Y_1\right) \\
&\times f^*\left(-\frac{R}{R'}X' - \frac{m'\lambda R}{p'}, Y_2\right) \\
&\times \tau_m\left(-\frac{Y'}{R'} - \frac{Y_1}{R}\right) \tau^*_{m'}\left(-\frac{Y'}{R'} - \frac{Y_2}{R}\right) \\
&\times \exp\left[\frac{2\pi i}{\lambda R_0}(Y_1 - Y_2)y_0\right] \mathrm{d}x_0 \mathrm{d}y_0. \qquad (8)
\end{aligned}
$$

With respect to the incoming illumination, we make the following assumptions:

$$
I(x_0, y_0) = 1, \qquad T(x_0, y_0) = T_x(x_0); \qquad (9)
$$

the second assumption implies that we use a rectilinear source grating. The function $T_x(x_0)$ is periodic in x_0 with period p.

With the change of variables $\eta = Y_1$, $Y_1 - Y_2 = q$, we perform the integration over y_0, which yields the δ function $\delta(q)$. The integration of Eq. (8) with respect to q now yields

$$
\begin{aligned}
&I_{\mathrm{tot}}(X', Y') \\
&\quad = \sum_m \sum_{m'} \iint T_x(x_0) \exp\left\{2\pi i\left(\frac{m - m'}{p'}\right)\left[\Delta x' - \left(\frac{R}{R_0}\right)x_0\right]\right\} \\
&\qquad \times f\left(-\frac{R}{R'}X' - \frac{m\lambda R}{p'}, \eta\right) f^*\left(-\frac{R}{R'}X' - \frac{m'\lambda R}{p'}, \eta\right) \\
&\qquad \times \tau_m\left(-\frac{Y'}{R'} - \frac{\eta}{R}\right) \tau^*_{m'}\left(-\frac{Y'}{R'} - \frac{\eta}{R}\right) \mathrm{d}\eta \, \mathrm{d}x_0. \qquad (10)
\end{aligned}
$$

The integration over x_0 of the periodic function $T_x(x_0)$ with period p yields a nonzero value only if the following condition is satisfied:

$$
p = \left(\frac{n}{m - m'}\right)\left(\frac{R_0}{R}\right)p', \qquad (11)
$$

where n is some integer $(m \neq m')$.

This condition says that, apart from a trivial magnification factor R/R_0, the periods of the source grating and the Ronchi grating should be matched to each other in some ratio $(m - m')/n$. If this matching condition is satisfied, the value of the integral equals $\mathcal{A}_n$, the complex amplitude of the nth diffraction order of the source grating. Before evaluating Eq. (10), we introduce a possible shift Δx_0 in the position of the source grating. A shift Δx_0 of G_S or a shift $\Delta x'$ of the Ronchi grating G_R makes it possible to alter the state of interference on the screen D and thus opens the way to applying multiexposure phase-stepping interferometry.[9]

We finally obtain the following for the total intensity distribution, apart from a multiplicative factor:

$$
\begin{aligned}
&I_{\mathrm{tot}}(X', Y') \\
&\quad = \sum_{n=-\infty}^{\infty} \mathcal{A}_n \exp\left\{\frac{2\pi i n}{p}\left[\Delta x_0 + \left(\frac{R_0}{R}\right)\Delta x'\right]\right\} \\
&\qquad \times \sum_m \int f\left(-\frac{R}{R'}X' - \frac{m\lambda R}{p'}, \eta\right) \\
&\qquad \times f^*\left(-\frac{R}{R'}X' + \frac{n\lambda R_0}{p} - \frac{m\lambda R}{p'}, \eta\right) \\
&\qquad \times \tau_m\left(-\frac{Y'}{R'} - \frac{\eta}{R}\right) \tau^*_{m - n[(R_0/R)(p'/p)]}\left(-\frac{Y'}{R'} - \frac{\eta}{R}\right) \mathrm{d}\eta. \qquad (12)
\end{aligned}
$$

If we inspect a single cross product that is due to two interfering terms, we derive the following expression from Eq. (12):

$$
\begin{aligned}
I_{m,m'}(X', Y') &= \mathcal{A}_{(m-m')[(R/R_0)(p/p')]} \\
&\times \exp\left[\frac{2\pi i(m - m')}{p'}\left(\frac{R}{R_0}\Delta x_0 + \Delta x'\right)\right] \\
&\times \int f\left(-\frac{R}{R'}X' - \frac{m\lambda R}{p'}, \eta\right) \\
&\times f^*\left(-\frac{R}{R'}X' - \frac{m'\lambda R}{p'}, \eta\right) \\
&\times \tau_m\left(-\frac{Y'}{R'} - \frac{\eta}{R}\right)\tau^*_{m'}\left(-\frac{Y'}{R'} - \frac{\eta}{R}\right)\mathrm{d}\eta, \qquad (13)
\end{aligned}
$$

where we have used for the index of $\mathcal{A}$ the value of n that satisfies the relation of Eq. (11). Note that the real value of the cross product is obtained by summing $I_{m,m'}$ and $I_{m',m}$. Such a partial sum might even be negative; it is only the full expression for I_{tot} that should be positive definite.

To avoid unwanted interference terms, we prefer a situation where only one cross term plus its complex conjugate contributes to the intensity on the detection screen. A good impression of the importance of various cross products is obtained when we evaluate the expressions:

$$C_{m,m'} = \int \tau_m(\eta)\tau^*_{m'}(\eta)\mathrm{d}\eta. \qquad (14)$$

On reducing Eq. (13) to this simplified version, we ignore the convolution effect present in Eq. (13), and we suppose that the value of a cross product is independent of the position (X', Y') on the detection screen. This is justified, since the functions τ_m are all very narrow with respect to the slowly varying pupil function $f(X', Y')$, and on using the simplified expression (14), we just neglect parasitic effects close to the border of the (displaced) functions $f(X', Y')$.

The evaluation of the cross products according to Eq. (14) is presented in Subsection 3.B and is treated in more detail in Appendix B.

B. Implementation of the Improved Ronchi Test

Having analyzed the formation of the Ronchi interferogram, we now describe in this subsection the measures taken to arrive at a Ronchi test that yields the interferogram of just two sheared pupil functions.

In the Ronchi test with an extended source, the entrance pupil is illuminated in a partially coherent way. The coherence function in the entrance pupil is obtained by means of a Fourier transform of the intensity function in the source plane (Zernike–van Cittert theorem[6]). Apart from a scaling factor, this coherence function is also found in the exit pupil of the optics to be tested. In the case of an extended source covered with a transmission grating (period p_S), the coherence function is periodic with a spacing Δ_c in the exit pupil given by

$$\Delta_c = \frac{\lambda R}{p'_S}, \qquad (15)$$

where p'_S is the period of the image of the source grating.

In Fig. 5 we have shown the coherence geometry in the exit pupil EP and the way in which the Ronchi grating with period p' is splitting up the outgoing wave into various diffraction orders. In the ideal case, we would like to have only first-order satellites in the exit pupil. However, with the use of binary gratings, higher-order satellites are generally present. Also, the Ronchi grating itself will generally show higher-order diffracted waves, and this leads to the ambiguous multiinterference pattern of the Ronchi test.

We propose to solve the ambiguity problem by the following two steps:

- $p' = 2p'_S$. This particular choice causes the Ronchi grating to diffract the waves coming from the coherent points Q_i over an angle corresponding to half of the distance Δ_c in the exit pupil. From Fig. 5 we see that, e.g., waves from the coherent points Q_0 and Q_{+1} overlap in a point P′, which, backprojected onto the exit pupil, is situated in P_0, exactly midway between Q_0 and Q_{+1}. In the Ronchi pattern, we thus observe the interference between the points Q_0 and Q_{+1} in a position midway, and, applied

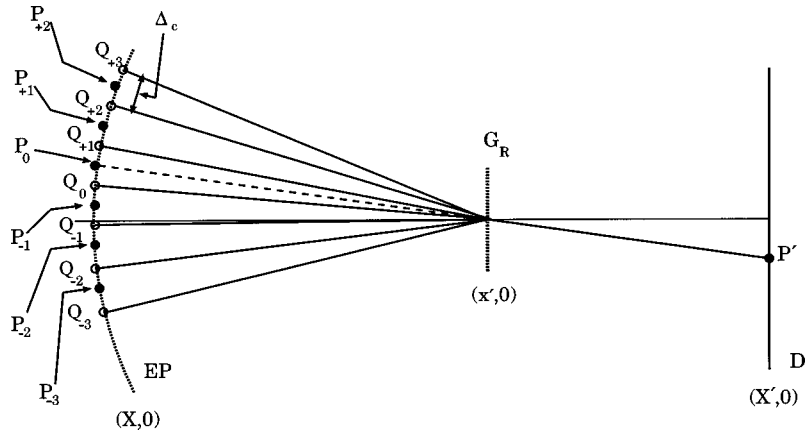

Fig. 5. View along the vertical direction of the periodic coherence distribution in the exit pupil EP of the optics (horizontal cross section with $Y = y' = Y' = 0$). The interference in a general point P′ is determined by, e.g., the odd orders from the Ronchi grating G_R of the points Q_0 and its coherent satellites Q_i. Further contributions in P′ originate from the even orders of the point P_0 and its coherent satellites P_i. The period p' of the Ronchi grating is twice the period p'_S of the projected source grating. Only the diffracted waves toward the point P′, conjugate with the point P_0 on the wavefront, have been shown. The auxiliary lens L has been omitted.

to all points Q_0, this is equivalent with the interference between two mutually shifted pupil functions.

• Introduction of a cosine-type binary grating. The suppression of unwanted interference cross products is essential for obtaining a linear Ronchigram. In general, the intensity in a point P′ is also influenced by, e.g., the interference between the zero order of P_0 itself and the minus second order of, e.g., the point P_{-1}, both generated by the Ronchi grating G_R. Further unwanted interferences in P′ are due to, e.g., the third order of Q_{+2}, the fifth order of Q_{+3}, the minus fourth order of P_{-2}, etc. All these unwanted coherent additions should be suppressed, leading to a clean, unambiguous Ronchigram.

We may conclude that a pure Ronchigram based on the interference of only two shifted wave fronts is possible both when the set of coherent satellites Q_m is strongly reduced and when the Ronchi grating itself preferably delivers only zero and first orders. This condition can be fulfilled with amplitude gratings having an analog cosine transmission function, but such gratings are not a realistic option in many applications. With the more standard binary gratings, higher orders are inevitable; the even orders can be more or less suppressed by choosing a duty cycle of 50%. In Section 3 we will show how an effective cosine grating can be simulated by using a binary structure and how extra measures can be taken to reduce further the residual amplitude of certain orders.

3. BINARY GRATING STRUCTURE WITH COSINE-TYPE BEHAVIOR

The parameter that is commonly used to reduce the magnitude of higher orders of a standard rectilinear binary grating is its duty cycle. By tuning the grating to a 50% duty cycle, one can suppress all even diffraction orders. However, for high-frequency gratings with a period approaching the wavelength of the light, it is generally not possible to suppress the even orders for both s and p polarization because the apparent duty cycle strongly depends on the state of polarization. Even if the even orders can be adequately suppressed, the amplitude of the odd orders will remain at an appreciable level. In Fig. 6 we have shown how two incoherent source points Q_1 and Q_2 contribute to the final interference pattern on the screen D. By the introduction of a cosine-type grating for G_R, the duty cycle of the Ronchi grating becomes y' dependent. A varying duty cycle implies varying amplitude and phase of the diffraction orders, which are all contributing to the total interference pattern at D. Taking into account the proper weighting with the amplitude and the phase of the diffraction orders, we may expect that the summed interferences between certain orders is nulled as a result of a mutual phase reversal when the source points have covered the full vertical cross section of the cosine-type grating.

To simulate the behavior of a cosine-type grating with a binary transmission structure, we have chosen the layout of Fig. 7; this type of grating we call a quasi-cosine grating. In Subsection 3.A we calculate the diffraction pattern of such a quasi-cosine binary grating. For the relevance of such a grating in the Ronchi test, it is important

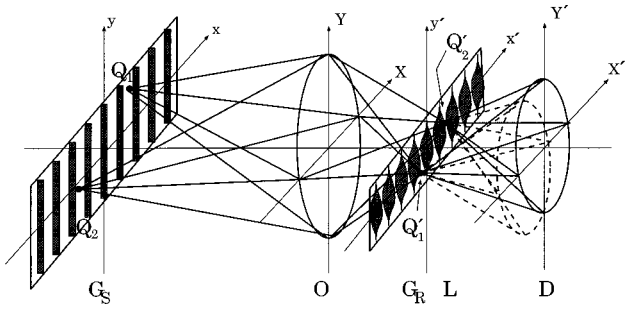

Fig. 6. Ronchi test carried out with a cosine-type grating. The state of interference on the detection screen depends on the varying duty cycle that is encountered by the incoherent source points Q when they are imaged onto the cosine grating (points Q′).

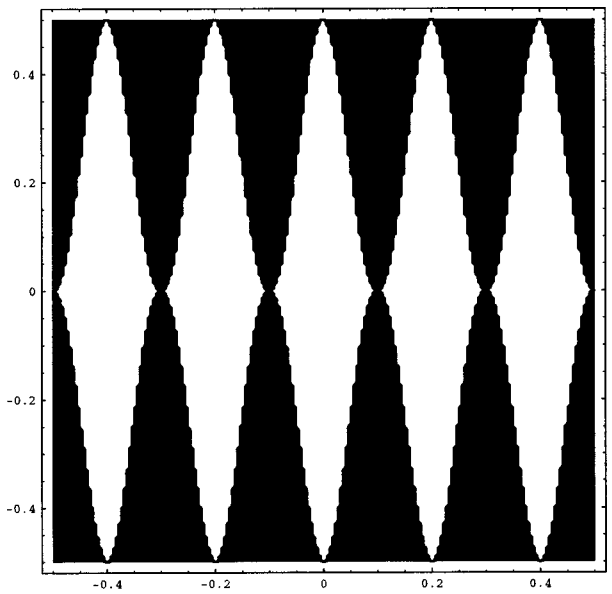

Fig. 7. Binary grating with quasi-cosine transmissive behavior. A section of a grating with five periods has been shown. Integrated along vertical lines, the transmission varies in a cosine manner. The period of the grating in the x' direction is p', and the extent in the y' direction is q'. The digitized appearance of the grating profile is an artifact that is due to the limited number of pixels used to represent the smooth profile. In a practical application, the ratio p'/q' will be much smaller than the value of 1/5 presented in the figure.

to show that the cross products of higher-order diffraction patterns with the lower orders (zero and first orders) are effectively zero. Only in this case can we claim to produce a Ronchi interferogram that is due to the interference of only two shifted pupil functions. The calculation of the cross products of diffraction orders will be the subject of Subsection 3.B.

A. Far-Field Diffraction Pattern of the Quasi-Cosine Grating

In the following analysis, we apply a Fourier transform to the transmission function of the quasi-cosine grating; optically, this transform is obtained as the complex amplitude distribution in the focal plane of the lens L (see Fig. 4). With use of the grating plane coordinates (x', y') and the far-field coordinates (X', Y'), the amplitude of

the far-field diffraction pattern of the function $t(x', y')$ in the focal plane of L is proportional to

$$A_t(X', Y') = \frac{1}{(2K+1)p'q'} \int_{-Kp'}^{Kp'} \int_{-q'/2}^{q'/2} t(x', y') \times \exp\left[\frac{2\pi i}{\lambda R'}(X'x' + Y'y')\right] dx'dy', \quad (16)$$

where the grating comprises $2K+1$ grating periods (length p') in the x' direction and has a height q' in the y' direction. The distance from the grating plane to the far-field observation region is again denoted by R'.

The binary transmission function $t_0(x', y')$ of an elementary (centered) period is given by

$$t_0(x', y') = \begin{cases} 1, & -\frac{q'}{4}\left[1 + \cos\left(2\pi \frac{x'}{p'}\right)\right] \leqslant y' \\ & < \frac{q'}{4}\left[1 + \cos\left(2\pi \frac{x'}{p'}\right)\right], \quad -\frac{p'}{2} \leqslant x \leqslant \frac{p'}{2}. \\ 0, & \text{elsewhere} \end{cases} \quad (17)$$

Equation (16) can be rewritten as

$$A_t(X', Y') = \frac{1}{(2K+1)p'q'} \sum_{k=-K}^{+K} \exp\left(2\pi i k \frac{Xp}{\lambda R'}\right) \times \int_{-p'/2}^{p'/2} \int_{-q'/2}^{q'/2} t_0(x', y') \times \exp\left[\frac{2\pi i}{\lambda R'}(X'x' + Y'y')\right] dx'dy'; \quad (18)$$

then, when we use the expression for $t_0(x', y')$, the final amplitude turns out to be (see Appendix A)

$$A_t(X', Y') = \frac{1}{2} \sum_m \left[\frac{J_m\left(\frac{\pi Y'q'}{2\lambda R'}\right)}{\frac{\pi Y'q'}{2\lambda R'}}\right] \times \sin\left[\frac{\pi}{2}\left(\frac{Y'q'}{\lambda R'} + m\right)\right] \times \operatorname{sinc}\left[\pi\left(m + \frac{X'p'}{\lambda R'}\right)\right] \times \frac{\operatorname{sinc}\left[\pi(2K+1)\left(\frac{X'p'}{\lambda R'}\right)\right]}{\operatorname{sinc}\left[\pi\left(\frac{X'p'}{\lambda R'}\right)\right]}. \quad (19)$$

The far-field amplitude consists of a number of diffraction orders and shows the well-known

$$\operatorname{sinc}[(2K+1)X'p'/\lambda R']/\operatorname{sinc}(X'p'/\lambda R')$$

pattern in the X' direction with peaks at the positions $X' = m\lambda R'/p'$. The amplitude of an order with order number m is given by the product of the first two factors of Eq. (19) after the summation sign. A standard rectilinear grating would have a $\operatorname{sinc}(Y'q'/\lambda R')$ profile in the Y' direction. Because of the y'-dependent modulation of the quasi-cosine grating, the far-field pattern is more complicated and generally extends over a larger distance. The Y'-dependent profile is given by the first two terms from Eq. (19). For the amplitude at $Y' = 0$, we find the following for the various diffraction orders:

$$A_t(0, 0) = 1/2,$$
$$A_t(\pm\lambda R'/p', 0) = 1/4,$$
$$A_t(\pm m\lambda R'/p', 0) = 0, \qquad |m| \geqslant 2. \quad (20)$$

The amplitude pattern around a diffraction peak at $(m\lambda R'/p', 0)$ is studied in more detail in Subsection 3.B.

B. Far-Field Cross Products of Diffracted Orders

When a quasi-cosine grating is used in a Ronchi setup, either as a source grating or as the proper analyzing Ronchi grating, the diffracted orders are superposed in the detection plane D. The amplitude pattern of diffracted orders is identical with respect to the X' coordinate but varies in the orthogonal Y' direction as a function of the order number m. The amplitude on the line $Y' = 0$ is given by Eqs. (20), but for a full cancellation of the unwanted interferences with higher orders we have to prove that the integral along Y' of the product of the amplitudes of two diffraction orders yields zero except for the cross product of the zero and first orders.

Replacing the quotient $Y'q'/\lambda R'$ by v, we evaluate the following expression for a cross product $C_{m,n}$ between two diffraction orders:

$$B_m(v) = \frac{1}{2}\left[\frac{J_m(\pi v/2)}{\pi v/2}\right]\sin[(\pi/2)(v+m)],$$
$$C_{m,n} = \int_{-\infty}^{+\infty} B_m(v)B_n(v)dv, \quad (21)$$

where it can be easily deduced that $C_{-m,n} = C_{m,-n} = C_{m,n}$.

In Appendix B we shall show that all $C_{m,n}$ can be evaluated:

$$C_{m,n} = \begin{cases} 0 & m+n \text{ odd},\ m,\ n = 1, 2,\ldots, \quad (22) \\ \dfrac{-2}{\pi^2}\left[\dfrac{1}{(n+m)^2-1}\right]\left[\dfrac{1}{(n-m)^2-1}\right] & \\ & m+n \text{ even},\ m,\ n = 1, 2,\ldots, \quad (23) \end{cases}$$

$$C_{0,1} = C_{1,0} = \frac{1}{8},$$

$$C_{0,n} = C_{n,0} = 0, \qquad n = 3, 5,\ldots, \tag{24}$$

$$C_{0,0} = \frac{1}{2} - \frac{2}{\pi^2},$$

$$C_{0,n} = C_{n,0} = \frac{-2}{\pi^2}\left(\frac{1}{n^2-1}\right)^2, \qquad n = 2, 4,\ldots . \tag{25}$$

For the contrast $c_{m,n}$ of an interfering term, we define

$$c_{m,n} = 2\frac{\mathcal{A}_{n'}C_{m,n}}{\mathcal{A}_0 C_{0,0}}, \qquad n' = (m-n)\frac{R}{R_0}\frac{p}{p'}, \tag{26}$$

and the relative contrast $r_{m,n}$ is given by

$$r_{m,n} = \frac{C_{m,n}}{C_{1,-1}}, \tag{27}$$

the ratio of the strengths of an unwanted interference term and the desired signal term $C_{1,-1}$.

From the expression for $C_{m,n}$, we conclude that one set of perturbing terms, the interferences of the zero order and the higher odd orders, is effectively suppressed by using a quasi-cosine grating. However, the terms $C_{0,n}$, with n even, are not fully suppressed, especially the $C_{0,2}$ term, which has a relative value with respect to $C_{0,0}$ of approximately 1/13. To eliminate this term, we have to apply an extra modification of the grating structure. We propose a grating sequence where the sections with their center points located at negative x' values are displaced over a distance $-p'/8$, whereas the sections on the positive side of the y' axis are shifted over a distance $+p'/8$. It can easily be shown that with this geometrical modification the grating orders are multiplied by a factor $\cos[(\pi/4)m(X'p'/\lambda R')]$, which eliminates the orders with order number $\pm 2, \pm 6,\ldots$; the next unwanted cross product ($C_{0,4}$) is left unchanged by this operation but is at a level of less than 0.003 with respect to $C_{0,0}$. We have to accept a change in the amplitude of the leading first orders by a factor of $(1/2)\sqrt{2}$ by this modification of the grating, and this reduces the modulation depth of the Ronchigram by a factor of 2. When phase-stepping procedures are used for the evaluation of the wave-front function, the final modulation depth of the interference pattern is of less concern than the inherent nonlinearity caused by the presence of higher-order interferences.

4. CONCLUSION

We have proposed an interferometric Ronchi test with an extended incoherent source that produces a pure shearogram of two shifted pupil functions. Because of the absence of interference between other than the first two orders, the shear ratio can be given an arbitrary small value. This avoids the complicated manufacture of high-frequency gratings when interferometry has to be applied to highly resolving systems with either a large numerical aperture or a small wavelength.

The linearity of the Ronchigram is obtained by giving the analyzing Ronchi grating a period that is twice the period of the source grating. In this way, only orders with an order difference of 2 are able to interfere. Harmful interferences are suppressed by using a specially designed binary grating with a cosine profile instead of a rectilinear profile. Such a profile is effective in suppressing the odd higher orders. When the grating is divided into two sections separated by a shift (offset) of a quarter-period, the second order is also suppressed, and a virtually perfect cosine grating is obtained. Our preferred implementation of the new Ronchi test is to use a standard rectilinear grating as the source grating and a quasi-cosine grating with a $p/4$ offset as the Ronchi grating. The binary Ronchi grating is achromatic with regard to the relative strengths of its diffracted orders. When the analyzing Ronchi grating is modified into a phase grating, its optimum performance becomes wavelength dependent; at a phase depth of π, the diffraction efficiency is greatly improved with respect to the binary amplitude grating.

APPENDIX A: DERIVATION OF THE FAR-FIELD AMPLITUDE PATTERN OF A QUASI-COSINE GRATING

Starting with the expression for the far-field amplitude of Eq. (18),

$$A_t(X', Y') = \frac{1}{(2K+1)p'q'}\sum_{k=-K}^{+K} \times \exp\left(2\pi i k \frac{X'p'}{\lambda R'}\right)\int_{-p'/2}^{p'/2}\int_{-q'/2}^{q'/2} t_0(x', y') \times \exp\left[\frac{2\pi i}{\lambda R'}(X'x' + Y'y')\right]dx'dy', \tag{A1}$$

we first perform the integration over y' by using the x'-dependent integration limits from Eq. (17):

$$A_t(X', Y') = \frac{1}{(2K+1)p'q'}\sum_{k=-K}^{+K}\exp\left(2\pi i k \frac{X'p'}{\lambda R'}\right) \times \int_{-p'/2}^{p'/2}\exp\left(2\pi i \frac{X'x'}{\lambda R'}\right)dx' \frac{\lambda R'}{2\pi i Y'} \times \left(\exp\left\{\frac{\pi i Y'q'}{2\lambda R'}\left[1+\cos\left(2\pi\frac{x'}{p'}\right)\right]\right\} - \exp\left\{\frac{-\pi i Y'q'}{2\lambda R'}\left[1+\cos\left(2\pi\frac{x'}{p'}\right)\right]\right\}\right). \tag{A2}$$

With the Jacobi–Anger[10] expression

$$\exp(ia\ \cos\ \theta) = \sum_{m=-\infty}^{+\infty} i^m J_m(a)\exp(im\theta), \qquad \text{(A3)}$$

and performing the integration over x', we obtain the expression

$$A_l(X',\ Y') = \frac{1}{2(2K+1)} \sum_{k=-K}^{+K} \exp\left(2\pi ik\ \frac{X'p'}{\lambda R'}\right) \times \sum_m \frac{J_m\left(\frac{\pi Y'q'}{2\lambda R'}\right)}{\frac{\pi Y'q'}{2\lambda R'}} \sin\left[\frac{\pi}{2}\left(\frac{Y'q'}{\lambda R'} + m\right)\right] \times \operatorname{sinc}\left[\pi\left(m + \frac{X'p'}{\lambda R'}\right)\right]. \qquad \text{(A4)}$$

The summation over k from $-K$ to $+K$, the number of grating sections, is done by using the expression for the sum of a geometric series, and this yields the final result of Eq. (19).

APPENDIX B: CALCULATION OF THE CROSS PRODUCTS OF THE GRATING ORDERS

We shall evaluate

$$C_{m,n} = \tfrac{1}{4} I_{m,n}, \qquad m,\ n = 0, 1,..., \qquad \text{(B1)}$$

where

$$I_{m,n} = 2\int_{-\infty}^{+\infty} J_m(x)J_n(x)\frac{\sin(\frac{1}{2}\ \pi m + x)\sin(\frac{1}{2}\pi n + x)}{x^2}\,dx = \int_{-\infty}^{+\infty} J_m(x)J_n(x) \times \frac{\cos[\frac{1}{2}\pi(m-n)] - \cos[\frac{1}{2}\pi(m+n) + 2x]}{x^2}\,dx. \qquad \text{(B2)}$$

We distinguish between the cases $m + n$ odd and $m + n$ even, according to which

$$I_{m,n} = \begin{cases} (-1)^p \int_{-\infty}^{+\infty} J_m(x)J_n(x)\ \dfrac{\sin 2x}{x^2}\,dx & m + n = 2p + 1 \qquad \text{(B3)} \\ (-1)^p \int_{-\infty}^{+\infty} J_m(x)J_n(x)\ \dfrac{(-1)^n - \cos 2x}{x^2}\,dx & m + n = 2p \end{cases}$$

$$\text{for } p = 0, 1,... . \qquad \text{(B4)}$$

Our first observation is that the functions $J_m(x)$, $m = 0, 1,...$, and $J_n(x)/x$, $n = 1, 2,...$, have Fourier transforms that vanish outside $|\omega| < 1$. Explicitly, see Ref. 11 (Eqs. 11.4.24 and 11.4.25 on p. 486):

$$\psi_m(\omega) := \int_{-\infty}^{+\infty} \exp(-i\omega x)J_m(x)\,dx = \frac{2(-i)^m T_m(\omega)}{(1-\omega^2)^{1/2}}\,B(\omega), \qquad \text{(B5)}$$

$$\phi_n(\omega) := \int_{-\infty}^{+\infty} \exp(-i\omega x)\ \frac{J_n(x)}{x}\,dx = \frac{2i}{n}\,(-i)^n(1-\omega^2)^{1/2}U_{n-1}(\omega)B(\omega), \qquad \text{(B6)}$$

where $m = 0, 1,...$ in Eq. (B5) and $n = 1, 2,...$ in Eq. (B6). In Eqs. (B5) and (B6), the T_m (U_n) are the Chebyshev polynomials (see Ref. 11, Chap. 22) of the first (second) kind and of degree $m(n)$, and $B(\omega)$ is given by

$$B(\omega) = \begin{cases} 1, & |\omega| < 1 \\ 0, & |\omega| \geqslant 1 \end{cases}. \qquad \text{(B7)}$$

Accordingly, when $m \geqslant 1$, $n \geqslant 1$, the functions $J_m(x)J_n(x)/x^2$ have Fourier transforms $(1/2\pi)\phi_m * \phi_n$ by the convolution theorem, and $\phi_m * \phi_n$ is continuous and vanishes for $|\omega| \geqslant 2$. It follows for $p = 1, 2,...$ that

$$I_{m,n} = \begin{cases} 0 & m + n = 2p + 1,\ m,\ n = 1, 2,... , \qquad \text{(B8)} \\ (-1)^{(m-n)/2}\int_{-\infty}^{+\infty} J_m(x)J_n(x)/x^2\ dx, & \\ = \dfrac{-8}{\pi}\left[\dfrac{1}{(n+m)^2-1}\right]\left[\dfrac{1}{(n-m)^2-1}\right], & \\ \qquad m + n = 2p,\ m,\ n = 1, 2,... . \qquad \text{(B9)} \end{cases}$$

For the last identity in Eq. (B9), we have used Ref. 12 [Eq. (551, 2b) on p. 202].

There remain the cases with at least one of m and n equal to zero. By symmetry of $I_{m,n}$, we may assume that $m = 0$.

For $n = 2p + 1$ odd we use in Eq. (B3) the representation

$$\frac{\sin 2x}{2x} = \frac{1}{4}\int_{-2}^{2} \exp(-i\omega x)\,d\omega. \qquad \text{(B10)}$$

We then obtain the following from Eqs. (B5) and (B6) by the convolution theorem:

$$I_{0,n} = \int_{-\infty}^{+\infty} J_0(x)J_n(x)\,\frac{\sin 2x}{x^2}\,\mathrm{d}x$$
$$= \frac{1}{2}\int_{-2}^{+2}\left[\int_{-\infty}^{+\infty} J_0(x)\,\frac{J_n(x)}{x}\exp(-i\omega x)\mathrm{d}x\right]\mathrm{d}\omega$$
$$= \frac{1}{4\pi}\int_{-2}^{+2}\left[\int_{-\infty}^{+\infty}\psi_0(\omega_1)\phi_n(\omega-\omega_1)\mathrm{d}\omega_1\right]\mathrm{d}\omega$$
$$= \frac{1}{4\pi}\int_{-\infty}^{+\infty}\psi_0(\omega_1)\mathrm{d}\omega_1\int_{-\infty}^{+\infty}\phi_n(\omega)\mathrm{d}\omega, \qquad \text{(B11)}$$

where in the last step we have used the fact that ψ_0 and ϕ_n vanish outside $|\omega| < 1$, so that $\int_{-2}^{+2}$ can be replaced by $\int_{-\infty}^{+\infty}$. The last expression in Eq. (B11) can be evaluated by using the inverse Fourier transforms

$$J_m(x) = \frac{1}{2\pi}\int_{-\infty}^{+\infty}\exp(i\omega x)\psi_m(\omega)\mathrm{d}\omega,$$
$$\frac{1}{x}J_n(x) = \frac{1}{2\pi}\int_{-\infty}^{+\infty}\exp(i\omega x)\phi_n(\omega)\mathrm{d}\omega, \qquad \text{(B12)}$$

and the result is (where δ_p is Kronecker's delta)

$$I_{0,2p+1} = \tfrac{1}{2}\pi\delta_p, \qquad p = 0, 1,\ldots. \qquad \text{(B13)}$$

We next consider $I_{0,n}$ with even $n \geqslant 2$. Then $J_n(x)/x^2$ has a Fourier transform that vanishes outside $|\omega| < 1$. Explicitly, one can show from Eq. (B6) and the elementary properties of the Chebyshev polynomials that for $n = 2, 3,\ldots,$

$$\int_{-\infty}^{+\infty}\exp(-i\omega x)\,\frac{J_n(x)}{x^2}\,\mathrm{d}x$$
$$= \frac{i^n}{n}[1-\omega^2]^{1/2}\left[\frac{1}{n+1}U_n(\omega) - \frac{1}{n-1}U_{n-2}(\omega)\right]$$
$$\times B(\omega) \qquad \text{(B14)}$$

As above, it follows that for even $n \geqslant 2$,

$$I_{0,n} = (-1)^{n/2}\int_{-\infty}^{+\infty}J_0(x)J_n(x)/x^2\mathrm{d}x = \frac{-8}{\pi}\left(\frac{1}{n^2-1}\right)^2 \qquad \text{(B15)}$$

[see again Ref. 12 [Eq. 551, 2b) on p. 202].

We finally evaluate $I_{0,0}$. Using the representation

$$\left(\frac{\sin x}{x}\right)^2 = \frac{1}{4}\int_{-2}^{2}(2-|\omega|)\exp(-i\omega x)\mathrm{d}\omega \qquad \text{(B16)}$$

and [see Eq. (B5)]

$$\int \exp(-i\omega x)J_0{}^2(x)\mathrm{d}x$$
$$= \frac{1}{2\pi}\int_{-\infty}^{+\infty}\psi_0(\omega_1)\psi_0(\omega-\omega_1)\mathrm{d}\omega_1$$
$$= \frac{2}{\pi}\int_{-\infty}^{+\infty}\frac{B(\omega_1)B(\omega-\omega_1)\mathrm{d}\omega_1}{(1-\omega_1{}^2)^{1/2}[1-(\omega-\omega_1)^2]^{1/2}}, \qquad \text{(B17)}$$

we obtain

$$I_{0,0} = 2\int_{-\infty}^{\infty}J_0{}^2(x)\left(\frac{\sin x}{x}\right)^2\mathrm{d}x$$
$$= \frac{1}{\pi}\int_{-2}^{2}(2-|\omega|)$$
$$\times\left\{\int_{-\infty}^{\infty}\frac{B(\omega_1)B(\omega-\omega_1)\mathrm{d}\omega_1}{(1-\omega_1{}^2)^{1/2}[1-(\omega-\omega_1)^2]^{1/2}}\right\}\mathrm{d}\omega. \qquad \text{(B18)}$$

The integral on the far right-hand side of Eq. (B18) can be evaluated by elementary means, and we obtain

$$I_{0,0} = 2\pi - 8/\pi. \qquad \text{(B19)}$$

This settles our last case.

ACKNOWLEDGMENTS

The authors thank Matthieu Visser and Martijn Dekker of Philips Research Laboratories for their helpful comments and criticism on the subject of this paper.

Address all correspondence to Joseph Braat at Department of Applied Physics, Delft University of Technology, Lorentzweg 1, 2628 CJ Delft, The Netherlands, or e-mail, braat@optica.tn.tudelft.nl.

REFERENCES

1. V. Ronchi, "Forty years of history of a grating interferometer," Appl. Opt. **3**, 437–451 (1964).
2. G. Toraldo di Francia, "Geometrical and interferential aspects of the Ronchi test," in *Optical Image Evaluation*, Natl. Bur. Stand. (U.S.) Circ. No. 256 (U.S. GPO, Washington, D.C., 1954).
3. D. Malacara, "Geometrical Ronchi test of aspherical mirrors," Appl. Opt. **4**, 1371–1374 (1965).
4. R. Barakat, "General diffraction theory of optical aberration tests from the point of view of spatial filtering," J. Opt. Soc. Am. **59**, 1432–1439 (1969).
5. A. Cornejo-Rodriguez, "Ronchi test," in *Optical Shop Testing*, 2nd ed., D. Malacara, ed. (Wiley, New York, 1992), pp. 321–365.
6. M. Born and E. Wolf, *Principles of Optics* (Pergamon, New York, 1980).
7. J. Schwider, "Single sideband Ronchi test," Appl. Opt. **20**, 2635–2642 (1981).
8. G. Leibbrandt, G. Harbers, and P. Kunst, "Wave-front analysis with high accuracy by use of a double-grating lateral shearing interferometer," Appl. Opt. **35**, 6151–6161 (1996).
9. K. Creath, "Wyko systems for optical metrology," in *Optical Shop Testing*, 2nd ed., D. Malacara, ed. (Wiley, New York, 1992), pp. 637–652.
10. G. Arfken, *Mathematical Methods for Physicists* (Academic, New York, 1985).
11. M. Abramowitz and I. Stegun, *Handbook of Mathematical Functions* (Dover, New York, 1970).
12. W. Groebner and N. Hofreiter, *Integraltafel, Volume II: Bestimmte Integrale*, 5th ed. (Springer, Vienna, 1973.